International Journal of Heat and Mass Transfer 52 (2009) 1240–1244

Contents lists available at ScienceDirect

International Journal of Heat and Mass Transfer

journal homepage: www.elsevier.com/locate/ijhmt

Effect of reduced specific heats of nanofluids on single phase, laminar internal forced convection

T.L. Bergman *

Department of Mechanical Engineering, The University of Connecticut, 191 Auditorium Road, Unit 3139, Storrs, CT 06269, USA

ARTICLE INFO

Article history:
Received 25 April 2008
Received in revised form 22 August 2008
Available online 22 October 2008

Keywords:
Nanofluid
Augmentation
Microchannel

ABSTRACT

Laminar, internal forced convection utilizing nanofluids is analyzed, incorporating experimentally-verified descriptions of the nanofluid's specific heat, and accounting for the dual effects of (i) increased thermal conductivity and (ii) reduced specific heat of the nanofluid relative to its base liquid. Heat transfer enhancement is quantified, and a dimensionless effectiveness is introduced to gage the nanofluid's performance relative to that of the pure, base liquid. It is shown that use of nanofluidic versions of pure liquids can either enhance or degrade thermal performance.

1. Introduction

Recently, considerable interest has emerged regarding the potential use of nanofluids as high performance coolants in a variety of applications [1–3]. The rationale for developing such fluids is the fact that most traditional liquids exhibit low thermal conductivity, and incorporation of nanoparticles into a mixture has led to impressive increases in the effective thermal conductivity of nanofluids, relative to that of the base liquids. A fundamental understanding of why the thermal conductivity increases, sometimes dramatically, has apparently not been achieved, but is receiving considerable research attention. An additional attribute of nanofluids is their relative stability (nanoparticles remain in suspension for a long time relative to larger particles) and hence, their purported suitability for use in microchannel cooling applications without clogging or surface erosion [2].

A contemporary review [3] includes a discussion of factors that might lead to the increased thermal conductivities of nanofluids. Yu et al. [3] also present a compilation of data from the literature, including reported values of nanofluid thermal conductivities as well as values of the Nusselt number for both laminar and turbulent internal flows using various nanofluids. Broadly speaking, more experimental and theoretical studies are needed before general heat transfer correlations can be developed that account specifically for the myriad of factors that ultimately determine heat transfer rates, such as particle size and shape, fluid temperature, fluid pH, and other parameters [3].

The paucity of experimental studies involving nanofluids in actual cooling applications has been noted in a recent review [2]. One exception is an investigation by Lee and Mudawar [4] who present temperature measurements associated with single- and two-phase heat transfer in microchannels using both pure water, and water seeded with Al_2O_3 nanoparticles. A dielectric fluid, HFE 7100, in both its conventional and nanofluidic form, is also considered. Notably, Lee and Mudawar (and a few other authors) take a holistic approach in assessing the efficacy of nanofluids as coolants, looking beyond the obvious benefit of increased thermal conductivity or Nusselt numbers. Specifically, they stress that although increases in the thermal conductivity will occur when nanoparticles are added to the base liquid, other properties are also affected such as the specific heat of the resulting nanofluid. Typically, the nanofluid's specific heat is smaller than that of the base fluid. Hence, for flow in a channel with a constant heat flux boundary condition, for example, nanofluids will *simultaneously* (i) reduce the temperature difference between the wall and the fluid because of the nanofluid's higher thermal conductivity, *and* (ii) increase the local mean nanofluid temperatures relative to mean temperatures associated with use of the base fluid, because of the nanofluid's smaller specific heat. Because of these competing effects, the *net* benefit in terms of reduced device (wall) temperatures associated with use of nanofluidic versions of conventional liquids is unknown.

Accompanying the experimental work, a simple analysis of heat transfer in a tube with constant heat flux conditions, specifically investigating the wall's thermal response to pure versus nanofluidic coolants, considering water and HFE 7100 as the two base fluids, is presented in [4]. The density of the two nanofluids (both fluids contain Al_2O_3 nanoparticles) was described by $\rho_{nf} = (1-\varphi)\rho_{bf} + \varphi\rho_p$, the viscosity was expressed using Einstein's model as

* Tel.: +1 860 486 2345; fax: +1 860 486 5088.
E-mail address: tberg@engr.uconn.edu

0017-9310/$ - see front matter © 2008 Elsevier Ltd. All rights reserved.
doi:10.1016/j.ijheatmasstransfer.2008.08.019

Nomenclature

c_p	specific heat (J/kg K)
D	tube diameter (m)
h	heat transfer coefficient (W/m^2 K)
k	thermal conductivity (W/m K)
L	tube length (m)
$\dot{m}$	total mass flow rate (kg/s)
Nu	Nusselt number, hD/k
q	heat rate (W)
q''	heat flux (W/m^2)
Re	Reynolds number, $4\dot{m}/\pi D\mu$
T	temperature (°C)
x	axial coordinate direction

Greek symbols

ε	effectiveness
μ	dynamic viscosity (N s/m^2)
ρ	density (kg/m^3)
φ	nanoparticle volume fraction

Subscripts

bf	base fluid
crit	critical value
CF	constant heat flux
CT	constant wall temperature
D	diameter
i	inlet
m	mean, mass-averaged quantity
nf	nanofluid
p	particle
s	surface or wall
v	volume-averaged quantity

$\mu_{nf} = \mu_{bf}(1 + 2.5\varphi)$, whereas the effective thermal conductivity of either nanofluid was based on the Hamilton–Crosser model

$$k_{nf} = \left[\frac{k_p + (n-1)k_{bf} - (n-1)\varphi(k_{bf} - k_p)}{k_p + (n-1)k_{bf} + \varphi(k_{bf} - k_p)}\right]k_{bf} \quad (1)$$

where $n = 3$ for the nominally-spherical, 36 nm diameter nanoparticles [4]. The main parameter of interest in [4], the specific heat, was described on a volume-averaged basis

$$c_{p,nf} = (1-\varphi)c_{p,bf} + \varphi c_{p,p} \quad (2)$$

The predictions and measurements of [4] suggest that there is negligible enhancement associated with use of nanofluidic versions of base coolants, in terms of reduced wall (device) temperatures, "bringing into question the overall merit of using nanofluids in microchannel heat sinks".

Motivated by the interest in nanofluids, experimental measurements of the specific heat of water-based Al_2O_3 nanofluids (similar to the fluid used in [4]) have been recently reported [5]. In short, the volume-averaged formulation of Eq. (2) yields poor prediction of measured specific heats. In contrast, a mass-averaged expression satisfies the first law of thermodynamics and is of the form

$$c_{p,nf} = \frac{\varphi(\rho c_p)_p + (1-\varphi)(\rho c_p)_{bf}}{\varphi\rho_p + (1-\varphi)\rho_{bf}} \quad (3)$$

Note the Eq. (3) matches the experimentally-measured values of the specific heat exceptionally well, and is recommended specifically for the nanofluid of interest here [5]. Importantly, the validity of Eq. (3) stands whether or not nanoscale effects on the solid's specific heat [6] are accounted for. Finally, note that Eq. (1) has been reported to slightly *overpredict* the thermal conductivity of water–Al_2O_3 nanofluids with spherical particles [7].

A review of the literature reveals that a small number of studies have specifically addressed (i) the offsetting effects of increased thermal conductivities and reduced specific heats of nanofluids, while (ii) simultaneously correctly describing the specific heat dependence on particle loading [8–10]. Therefore, the objective of this study is to correct and extend the analysis presented by Lee and Mudawar by including the proper description of the specific heat of the nanofluid, replacing Eq. (2) with Eq. (3). In doing so, it will be shown that for particular channel lengths and operating conditions (mass flow rates) involving specific fluids, nanofluidic versions of pure liquids can lead to pronounced augmentation *or degradation* of thermal performance. Attention is limited to laminar flow since fully turbulent conditions are seldom encountered in microchannel heat transfer applications.

2. Analysis and results

2.1. Constant wall heat flux

Consider a circular tube of diameter $D = 0.2$ mm and $L = 100$ mm that imparts a constant heat flux ($q'' = 20$ kW/m^2) to a flowing fluid that is characterized by an inlet temperature of $T_{m,i} = 30$ °C. The specified coolant mass flow rate ($\dot{m} = 0.1\times 10^{-3}$ kg/s) leads to laminar conditions for the water-based nanofluid (for example, $Re_D = 798$ for pure water for these conditions). The hydrodynamic and thermal entrance lengths are negligibly short, so the analytical value of the Nusselt number ($Nu_D = 4.36$) is specified.

The axial mean temperature distribution of the fluid is determined by way of a simple energy balance, incorporating the definition of the Nusselt number, and assuming constant properties. That is

$$T_m(x) = T_{m,i} + \frac{q_s''\pi Dx}{\dot{m}c_{p,nf}}; \quad q_s'' = \frac{Nu_D k_{nf}}{D}[T_s(x) - T_m(x)] \quad (4a,b)$$

Properties of base fluids ($\varphi = 0$) and a representative nanofluid ($\varphi = 0.05$) are listed in Table 1.

Predictions of the axial mean and wall temperature distributions using water- and HFE 7100-based nanofluids with $\varphi = 0$ and 0.05 are presented in Fig. 1a and b, respectively. For $\varphi = 0.05$, two predictions are reported, one using Eq. (2) and the other using Eq. (3).

For water–Al_2O_3 (Fig. 1a) use of the recommended mass-averaged specific heat formulation, Eq. (3), leads to larger values of

Table 1
Fluid properties 4,5.

	$\varphi = 0$ (pure fluid)	$\varphi = 0.05$ (nanofluid)
Water base		
k_{nf}/W/m K	0.603	0.693
ρ_{nf}/kg/m^3	995.7	1126
μ_{nf}/N s/m^2	797.7×10^{-6}	897.4×10^{-6}
$c_{p,nf,v}$/J/kg K	4183	4012
$c_{p,nf,m}$/J/kg K	4183	3637
HFE 7100 base		
k_{nf}/W/m K	0.0678	0.0784
ρ_{nf}/kg/m^3	1455	1563
μ_{nf}/N s/m^2	655.6×10^{-6}	737.6×10^{-6}
$c_{p,nf,v}$/J/kg K	1193	1172
$c_{p,nf,m}$/J/kg K	1193	1144

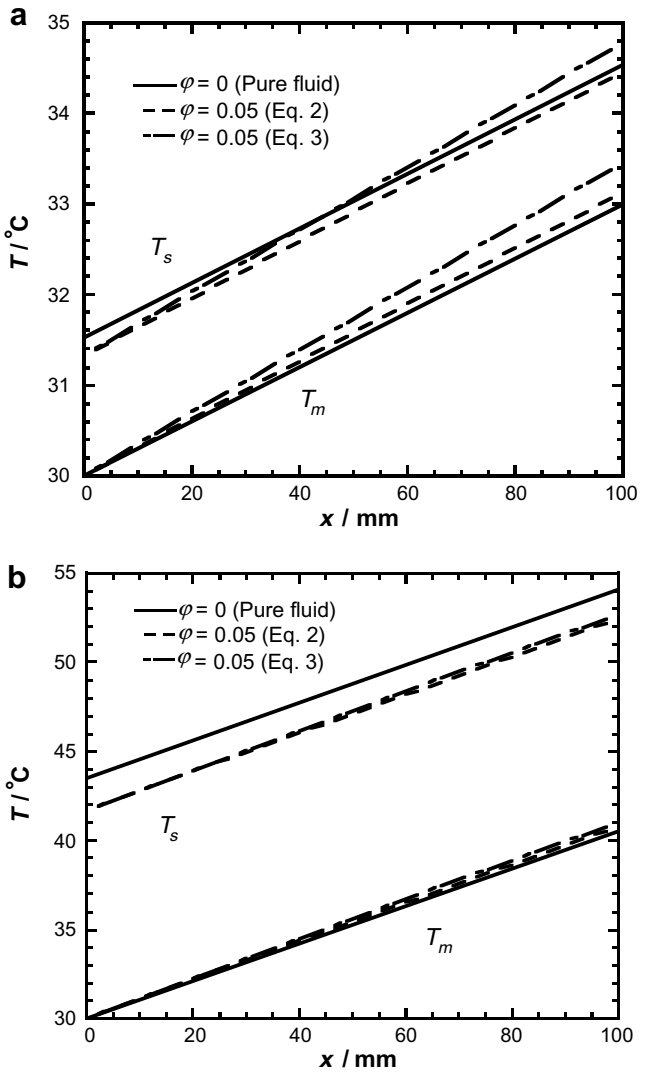

Fig. 1. Axial mean fluid and wall temperature distributions for (a) water–Al_2O_3 nanofluid and (b) HFE 7100–Al_2O_3 nanofluid using volume- and mass-averaged specific heat formulations with constant heat flux conditions.

the local mean fluid temperatures for $\varphi = 0.05$, relative to predictions based upon the volume-averaged specific heat, Eq. (2). This is expected, since Eq. (3) yields a smaller specific heat than Eq. (2). Moreover, close inspection of the water-based nanofluid with $\varphi = 0.05$ (Fig. 1a) indicates that, although differences between the wall temperature and mean temperature are smaller for the nanofluid relative to the pure fluid due to its higher thermal conductivity, approximately midway down the length of the tube the wall temperatures associated with the nanofluid using Eq. (3) begin to exceed those associated with the pure fluid, indicating that the nanofluid is *degrading* thermal performance. Degradation, in terms of higher wall temperatures, is not predicted when Eq. (2) is used. Similar behavior is noted in Fig. 1b, although the surface temperatures associated with the HFE 7100-based nanofluids never exceed the surface temperatures associated with the pure fluid, for the conditions of this example.

Motivated by the predictions shown in Fig. 1a, general guidelines are now developed to delineate between heat transfer (i) augmentation and (ii) degradation associated with use of nanofluids in single phase, laminar internal forced convective flow.

An energy balance on the fluid in the entire tube, coupled with application of Newton's law of cooling, yields the following expression for the ratio of the maximum overall temperature difference (the difference between the wall temperature at the tube exit and the fluid temperature at the tube inlet) to the overall heat rate, a figure of merit in any cooling application

$$\frac{T_s(x=L)-T_{m,i}}{q}=\frac{1}{\pi}\left[\frac{1}{Nu_D k_{\mathrm{nf}} L}+\frac{\pi}{\dot{m}c_{p,\mathrm{nf}}}\right] \tag{5}$$

To minimize wall (device) temperatures, it is therefore necessary to minimize the bracketed term of Eq. (5). Multiplying the bracketed term by the tube length, L, provides an alternative expression that may be minimized, and reduces the number of independent variables to (i) the volume fraction of nanoparticles, φ (which, in turn, yields values of k_{nf} and $c_{p,nf}$) and (ii) the ratio of the tube length to the mass flow rate, $L/\dot{m}$. Considering base case conditions to be associated with use of a specific base fluid, a new dimensionless nanofluid effectiveness, ε, for a particular nanofluidic version of the base liquid may be easily derived for single phase laminar flow with constant heat flux conditions and is

$$\varepsilon_{\mathrm{CF}}=1-\frac{(T_s(x=L)|_{\mathrm{nf}}-T_{m,i})}{(T_s(x=L)|_{\mathrm{bf}}-T_{m,i})}=1-\frac{(1/k_{\mathrm{nf}})+(L/\dot{m})(\pi Nu_D/c_{p,\mathrm{nf}})}{(1/k_{\mathrm{bf}})+(L/\dot{m})(\pi Nu_D/c_{p,\mathrm{bf}})} \tag{6}$$

This effectiveness is a quantitative measure of the thermal performance of the nanofluid, relative to the performance of the base fluid. An effectiveness greater than zero is desirable, and is associated with a reduction in the maximum wall (device) temperature in response to use of a nanofluidic version of a base fluid for a given heat rate. An effectiveness less than zero is undesirable, and is associated with an increase in the maximum wall temperature using the nanofluid.

Fig. 2a shows the effectiveness of a water–Al_2O_3 nanofluid using the specific heat formulation of Eq. (3). Obviously, there is no nanofluidic augmentation or degradation associated with pure water ($\varphi = 0$) and $\varepsilon_{\mathrm{CF}} = 0$ for any operating condition. For the example of Fig. 1a, $L/\dot{m} = 10^3$ m s/kg, $\varphi = 0.05$, and $\varepsilon_{\mathrm{CF}} = 1 - (T_s(x=L) - T_{m,i})_{\mathrm{nf}}/(T_s(x=L) - T_{m,i})_{\mathrm{bf}} = 1 - (34.78\ ^\circ\mathrm{C} - 30\ ^\circ\mathrm{C})/(34.53\ ^\circ\mathrm{C} - 30\ ^\circ\mathrm{C}) = -0.056$, the same as predicted with the expression involving the properties of the base and nanofluids of Eq. (6), and as shown in Fig. 2a. For short tubes or high mass flow rates (small $L/\dot{m}$), mean fluid temperatures do not increase as much as for large $L/\dot{m}$. For small $L/\dot{m}$, the thermal resistance between the local wall temperature and local mean temperature dominates, and the thermal performance is enhanced with use of the nanofluid due to its high thermal conductivity, with maximum tube wall temperatures being reduced by approximately 8% for $L/\dot{m} = 100$ m s/kg and $\varphi = 0.05$. The augmentation at small $L/\dot{m}$ is reduced as φ is decreased, as expected. Alternatively, for longer tubes or lower mass flow rates (large $L/\dot{m}$), the undesirable influence of the reduced specific heat of the nanofluid begins to dominate the beneficial effects associated with its higher thermal conductivity, and degradation in the thermal performance is noted. For example, maximum tube wall temperatures increase by nearly 15% for $L/\dot{m} = 10^4$ m s/kg and $\varphi = 0.05$ if the nanofluid is used in lieu of the base fluid.

Regardless of the nanoparticle volume fraction, a distinct value of $L/\dot{m} \approx 500$ m s/kg emerges. Below this value, augmentation always occurs with this particular nanofluid and physical system, and above this value thermal degradation is always induced. Since a complete understanding of the thermal conductivities (or convection coefficients) of nanofluids has apparently not yet been achieved, the limiting case of $\varphi = 0.05$, $k_{\mathrm{nf}} \to \infty$ (or $h \to \infty$) is shown as the curved dashed line in Fig. 2a. *If* it were feasible to blend the ideal water–Al_2O_3 nanofluid possessing an *infinite* thermal conductivity (or infinite convection coefficient), its performance would be surpassed by pure water for $L/\dot{m}$ values greater than approximately 3000 m s/kg due to the specific heat reduction.

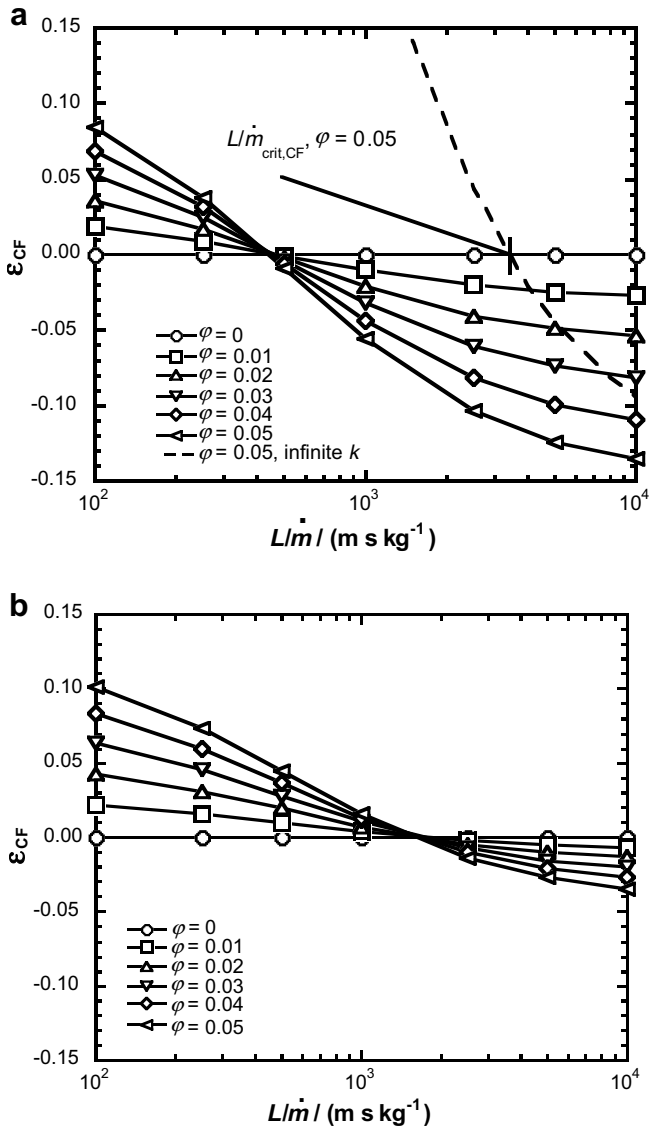

Fig. 2. Nanofluid effectiveness for water–Al_2O_3 nanofluid using (a) mass-averaged specific and (b) volume-averaged specific heat formulations with constant heat flux conditions.

Setting $\varepsilon_{CF} = 0$ and $k_{nf} \to \infty$ in Eq. (6), a specific relationship for $L/\dot{m}|_{crit,CF}$ may be derived,

$$L/\dot{m}|_{crit,CF} = \frac{1}{\pi N u_D k_{bf}} \left[\frac{1}{1/c_{p,nf} - 1/c_{p,bf}} \right] \tag{7}$$

which yields $L/\dot{m}|_{crit,CF} = 3370$ m s/kg (represented by the short vertical line of Fig. 2a) for the $\varphi = 0.05$ case. Use of nanofluidic versions of the base liquid at $L/\dot{m}$ values greater than $L/\dot{m}|_{crit,CF}$ would, in general, never be desirable.

Predictions of the effectiveness based upon the (incorrect) use of Eq. (2) are included in Fig. 2b. Because Eq. (2) under-predicts the reduction of the specific heat of the nanofluid (Table 1), its use yields an optimistic prediction of the nanofluid's effectiveness, with positive effectiveness values being over-predicted over a large range of $L/\dot{m}$ relative to Fig. 2a, and negative effectiveness values being under-predicted relative to Fig. 2a. For the example of Fig. 1a, $L/\dot{m} = 10^3$ m s/kg, $\varphi = 0.05$, and $\varepsilon = 1 - (33.46\,^{\circ}\text{C} - 30\,^{\circ}\text{C})/(34.53\,^{\circ}\text{C} - 30\,^{\circ}\text{C}) = +0.0155$, consistent with Fig. 2b. The distinct value of $L/\dot{m}$ below which augmentation occurs and above which degradation is noted ($\approx$1500 m s/kg) is approximately three times larger than the value of Fig. 2a.

For purposes of comparison, results for HFE 7100–Al_2O_3 nanofluids are presented in Fig. 3. Since $(k_{nf}/k_{bf})/(c_{p,nf}/c_{p,bf})$ is greater for the HFE-based nanofluid than the water-based fluid (Table 1), only a small part of the operating range ($L/\dot{m} \geqslant 5000$ m s/kg) exhibits degradation of thermal performance (Fig. 1a). If, however, the incorrect expression is used for the specific heat (Eq. (2), Fig. 3b), pronounced degradation is not predicted to occur for any operating condition in the range of interest.

Finally, for either the water- or HFE 7100-based nanofluids, an alternative comparison might be to adjust the flow rate of the nanofluid so that the pressure drop along the tube length is the same as that associated with use of the base fluid. For the water-based nanofluid over the range $\varphi = 0 - 0.05$, this would permit an increase in the mass flow rate of the nanofluid of less than 0.52%, which, by inspection of Fig. 2a, would have a negligible effect on its thermal performance relative to the pure fluid. On the other hand, for the HFE 7100-based nanofluid, the mass flow rate of the nanofluid would have to be decreased by approximately 5%, further increasing the

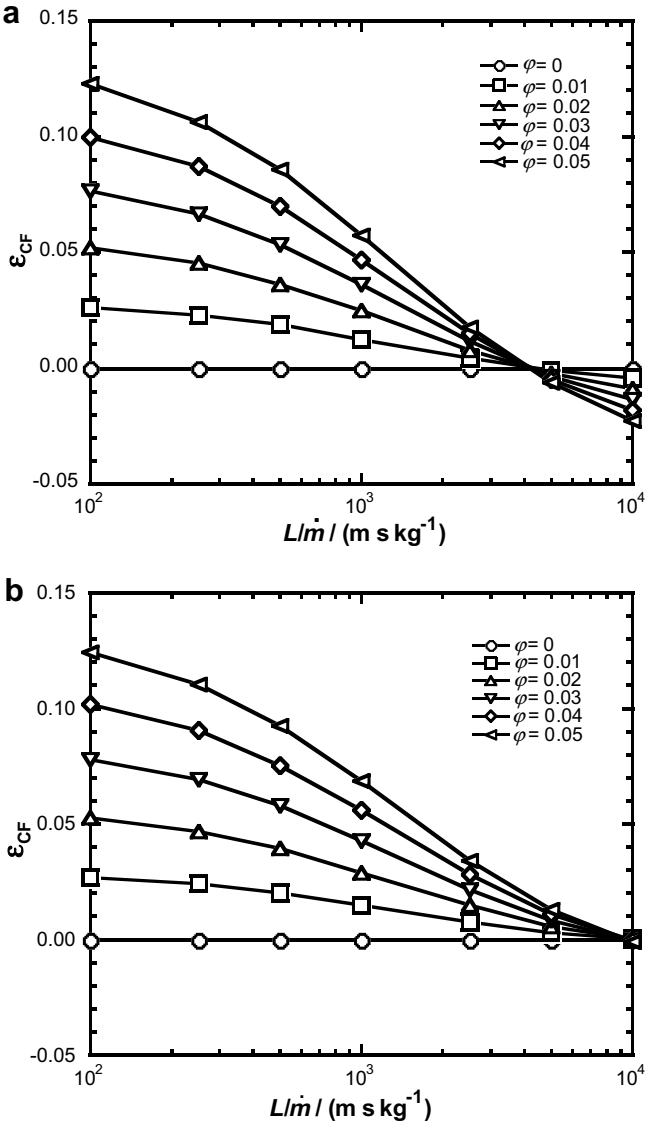

Fig. 3. Nanofluid effectiveness for HFE 7100–Al_2O_3 nanofluid using (a) mass-averaged specific and (b) volume-averaged specific heat formulations with constant heat flux conditions.

mean fluid and wall temperatures that respond to the nanofluid relative to those that evolve from use of the base liquid.

2.2. Constant wall temperature

The case of constant wall temperature is included for completeness. Again, a constant property fluid with negligible entrance lengths is considered. For this situation, the mean fluid temperature at the tube exit, and the total heat transfer to the fluid may be expressed as [11]

$$\frac{T_s - T_m(x)}{T_s - T_{m,i}} = \exp\left(-\frac{\pi Nu_D k_{nf}}{\dot{m} c_{p,nf}} x\right); \quad q = \dot{m} c_{p,nf}(T_m(x) - T_{m,i}) \tag{8a, b}$$

where $Nu_D = 3.66$. Eq. (8) can be manipulated to yield a new expression for the effectiveness associated with use of the nanofluid under constant wall temperature conditions

$$\varepsilon_{CT} = \frac{q_{nf}}{q_{bf}} - 1 = \frac{c_{p,nf}\left[1 - \exp\left(-\frac{\pi Nu_D k_{nf}}{c_{p,nf}} \cdot \frac{L}{\dot{m}}\right)\right]}{c_{p,bf}\left[1 - \exp\left(-\frac{\pi Nu_D k_{bf}}{c_{p,bf}} \cdot \frac{L}{\dot{m}}\right)\right]} - 1 \tag{9}$$

The effectiveness of water–Al_2O_3 nanofluid is shown in Fig. 4. As for the constant heat flux case, the effectiveness is high at small values of $L/\dot{m}$, suggesting that use of nanofluidic versions of the base fluid will lead to greater heat transfer rates for short tubes or high mass flow rates. At large values of $L/\dot{m}$, however, the effectiveness is reduced and asymptotic behavior, associated with $T_m(x = L) \to T_s$ is noted. The transition between augmentation and degradation occurs at $L/\dot{m} \approx 650$. The limiting case of $\varphi = 0.05$, $k_{nf} \to \infty (h \to \infty)$ is shown as the curved dashed line, with the effectiveness becoming independent of the thermal conductivity at large values of $L/\dot{m}$. Setting $\varepsilon_{CT} = 0$ and $k_{nf} \to \infty$ in Eq. (9) yields a specific relationship for $L/\dot{m}|_{crit,CT}$

$$L/\dot{m}|_{crit,CT} = -\frac{c_{p,bf} \ln[1 - c_{p,nf}/c_{p,bf}]}{\pi Nu_D k_{bf}} \tag{10}$$

For $\varphi = 0.05$, $L/\dot{m}|_{crit,CT} = 1228$ m s/kg, as identified in Fig. 4 by the short vertical solid line. For this case, operation at $L/\dot{m}$ values greater than $L/\dot{m}|_{crit,CT}$ would, in general, not be desirable.

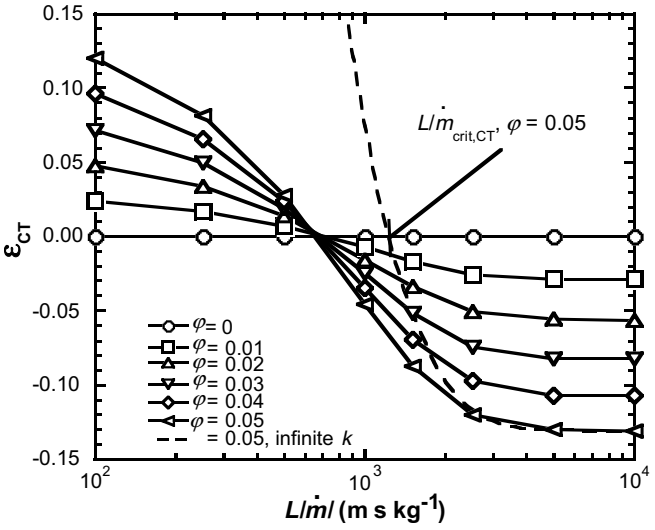

Fig. 4. Nanofluid effectiveness for water–Al_2O_3 nanofluid with constant wall temperature boundary conditions.

3. Summary and conclusions

Using simple analyses incorporating an experimentally-validated expression for the specific heat of water–Al_2O_3 nanofluids, it has been shown that nanofluids characterized by increased thermal conductivity and reduced specific heat, relative to their base fluids, can augment ($\varepsilon > 1$), reduce ($\varepsilon = 1$) or have no effect ($\varepsilon = 0$) on the thermal performance of single phase, laminar microchannel heat transfer. This is because the degree of enhancement or degradation is geometry- and flow rate dependent, as shown for the simple case of a channel of varying length or mass flow rate. New expressions for the dimensionless effectiveness of a nanofluidic version of a base liquid are derived for both constant heat flux and constant temperature conditions. Critical values of $L/\dot{m}$ have also been derived using conventional values of the Nusselt number for laminar internal forced convection. Because Eqs. (7) and (10) are based upon the conservation of energy principle and expressed in terms of the Nusselt number, they may be used to refine values of $L/\dot{m}|_{crit}$ as improved expressions for Nu_D become available.

Extrapolating the observations made here to more complex geometries and applications, one may anticipate that the potential benefits of using nanofluidic coolants in single phase flow can be claimed only if the specific operating conditions and dimensions of the heat transfer device in which the fluid will be used (or in which experiments will be performed) are known. In other words, a particular nanofluid might work well in one application (or yield encouraging results in one laboratory), but the same nanofluid would be a poor choice for use in a different application (or may yield discouraging results in a second laboratory).

Finally, inclusion of correct expressions for the specific heats of nanofluids is critical in assessing their efficacy, as demonstrated here. While attention has been focused on increasing the thermal conductivities of fluids by adding a second, nanoparticulate phase, or to increasing heat transfer coefficients and Nusselt numbers in convective situations using the resulting nanofluids, significant benefits might also be realized by blending nanofluids in a manner to increase the effective specific heat of the resulting mixture.

Acknowledgements

The author wishes to thank Amir Faghri and Ranga Pitchumani of the University of Connecticut for their helpful suggestions.

References

[1] J.A. Eastman, S.R. Phillpot, S.U.S. Choi, P. Keblinski, Thermal transport in nanofluids, Annu. Rev. Mater. Res. 34 (2004) 219–246.
[2] S.K. Das, S.U.S. Choi, H.E. Patel, Heat transfer in nanofluids – a review, Heat Transfer Eng. 27 (10) (2006) 3–19.
[3] W. Yu, D.M. France, J.L. Routbort, S.U.S. Choi, Review and comparison of nanofluid thermal conductivity and heat transfer enhancements, Heat Transfer Eng. 29 (5) (2008) 432–460.
[4] J. Lee, I. Mudawar, Assessment of the effectiveness of nanofluids for single-phase and two-phase heat transfer in micro-channels, Int. J. Heat Mass Transfer 50 (2007) 452–463.
[5] S.-Q. Zhou, R. Ni, Measurement of the specific heat capacity of water-based Al_2O_3 nanofluid, Appl. Phys. Lett. 92 (2008) 093123.
[6] L. Wang, Z. Tan, S. Meng, D. Liang, G. Li, Enhancement of molar heat capacity of nanostructured Al_2O_3, J. Nanoparticle Res. 3 (2001) 483–487.
[7] S. Lee, S.U.S. Choi, S. Li, J.A. Eastman, Measuring thermal conductivity of fluids containing oxide nanoparticles, J. Heat Transfer 121 (1999) 280–289.
[8] R. Chein, G. Huang, Analysis of microchannel heat sink performance using nanofluids, Appl. Thermal Eng. 25 (2005) 3104–3114.
[9] T.-H. Tsai, R. Chein, Performance analysis of nanofluid-cooled microchannel heat sinks, Int. J. Heat Fluid Flow 28 (2007) 1013–1026.
[10] S. Zeinali Heris, M. Nasr Esfahany, G. Etemad, Numerical investigation of nanofluid laminar convective heat transfer through a circular tube, Numer. Heat Transfer A 52 (2007) 1043–1058.
[11] F.P. Incropera, D.P. DeWitt, T.L. Bergman, A.S. Lavine, Fundamentals of Heat and Mass Transfer, sixth ed., Wiley, Hoboken, 2007.